

# THREE-DIMENSIONAL RESPONSE OF A PILE GROUP DUE TO TUNNEL ADVANCEMENT AT DIFFERENT C/D RATIOS

M. A. Soomro

*Quaid-e-Awam University of Science & Technology, Sindh, Pakistan*

D. Mašín

*Charles University in Prague, Czech Republic*

C. W. W. Ng

*Hong Kong University of Science & Technology, HKSAR*

**ABSTRACT:** Tunnels are often preferred for underground transportation systems in densely populated areas. It is almost inevitable to excavate a tunnel close to existing pile foundations in these areas. Since many previous studies mainly focus on the responses of single piles subjected to tunnelling, the effects of the tunnelling on pile groups are not well understood. In this study, two three-dimensional centrifuge tests were carried out to investigate settlement and load transfer mechanism of a pile group subjected to tunnelling at two critical locations relative to the pile group, namely next to (Test T) and below the toe of the pile group (Test B). Moreover, numerical back-analyses of the centrifuge tests are conducted by using a hypoplastic model, which takes small-strain stiffness into account. The tunnelling in test T resulted in the largest transverse tilting (of 0.2%) but the smallest settlement of the pile group under a working load. This is because the second tunnelling caused significant non-uniform change in vertical effective stress underneath the four piles in the group. On the contrary, the tunnelling below the pile group toe (i.e. test B) caused the smallest tilting but the largest settlement of the pile group (4.3% of pile diameter) and substantial mobilisation of shaft resistance. This is attributable to the most significant and uniform loss of toe resistance of each pile in the group resulting from stress relief from the tunnelling. Two distinct load transfer mechanisms can be identified in the pile group, namely downward load transfer in test T and upward load transfer in test B.

## 1. INTRODUCTION

The rapidly increasing demand for underground transportation systems in urban areas has been driving the construction of tunnels which are possibly excavated adjacent to existing piles. It is well recognised that the capacity of a pile group depends on mobilised stresses in the ground, while tunnelling is essentially a stress release process. Therefore, it is vital to investigate the adverse effects of tunnelling on existing pile foundations.

A number of field studies and centrifuge model tests have investigated this problem (Bezuijen and van der Schrier, 1994; Loganathan et al. 2000; Jacobsz et al. 2004; Lee and Chiang, 2007; Marshall and Mair, 2011; Ng and Lu, 2013; Ng et al. 2013; Soomro et al. 2015). They all concluded that tunnelling adjacent to existing pile foundations resulted in additional axial load of piles and pile settlement, the magnitudes of which likely depended on the relative locations of tunnel and pile. However, most of the previous studies have focused on the effects of tunnelling on single piles, which are only relevant to small bridge piers. Much less attention has been paid to the effects of tunnelling on pile groups, which are normally used to support high-rise buildings. It is likely that tunnelling adjacent to an existing pile group would result in complicated load transfer within each pile in the group, as well as load redistribution among the piles. Moreover, the piles in a group would experience differential settlement (tilting). Loganathan et al. (2000) carried out three centrifuge tests to investigate the effects of tunnelling (at three different depths) on the settlement, lateral movement and bending moment of a 2×2 pile group. Tilting, load transfer (within each pile) and load redistribution (among the four piles in the group), however, were not the focus of their study.

With the prime objective of investigating the effects of the tunnel location relative to an axially loaded 2×2 pile group, two three-dimensional centrifuge experiments were carried out in dry sand. The only variable that differed between the two tests was buried depth of the tunnels, which were located either

next to (Test T) or below the toe (Test B) of the pile group. The centrifuge tests were back-analysed by three-dimensional finite element analyses, in which a hypoplastic constitutive soil model was employed. Measured and computed results are compared and interpreted, with particular attention paid to settlement and load transfer mechanism of the pile group due to the tunnelling.

## 2. THREE-DIMENSIONAL CENTRIFUGE MODEL TESTS

### 2.1. SET UP OF CENTRIFUGE MODELLING

The centrifuge tests were carried out at the Geotechnical Centrifuge Facility of the Hong Kong University of Science and Technology (Ng, 2014). The centrifuge has a capacity of 400 g-ton, with an arm radius of 4.2 m. The test was conducted at an acceleration of 40 g.

Figure 1 shows the elevation view of the two tests (Test T and Test B), which are intended to investigate the responses of a 2x2 pile group due to tunnelling near and below the toe of the pile group. The diameter of each model tunnel (D) is 152 mm (6 m in prototype). Cover-to-diameter ratios (C/D) of the tunnels in test T and B are 2.7 and 3.7, respectively. The horizontal distance from the centerline of the tunnel to the nearest pile is 0.75D. All four piles were rigidly connected to a 130 mm × 130 mm × 20 mm pile cap. A dead weight of 8.6 kg (corresponding to 5.5 MN in prototype scale) was placed on the top of pile cap to simulate working load applied to the pile group. For determination this working load, more details are given by Ng et al. (2014).

Linear variable differential transformers (LVDTs) were installed at various places on the dead weight to measure settlement of the pile group (by “L1”), and transverse tilting of the pile group (deduced from measurement of “L2” and “L3”).

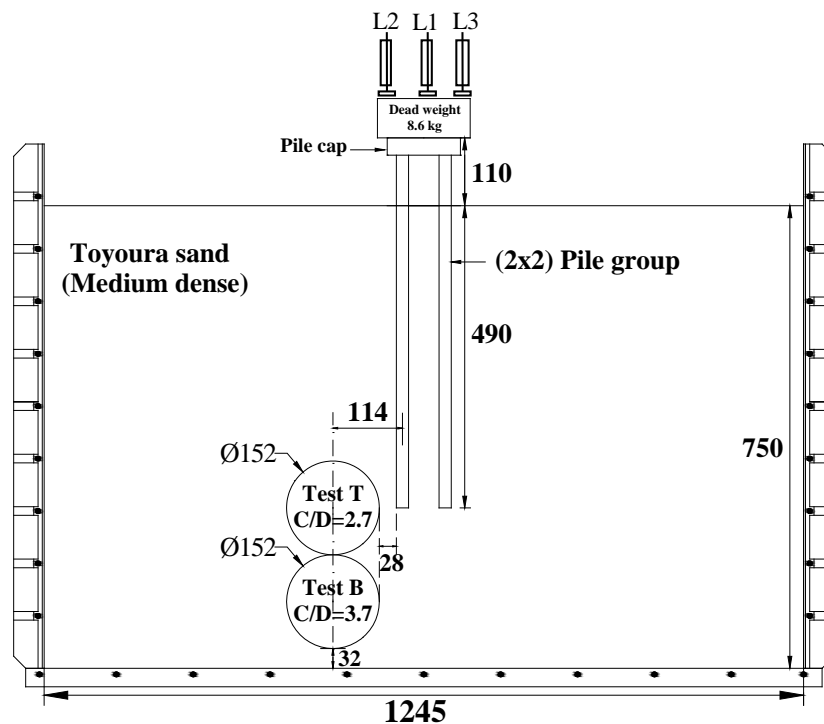


Figure 1: Configuration of centrifuge tests (i.e. Test T & Test B) (All dimensions are in mm)

### 2.2. IN-FLIGHT SIMULATION OF TUNNEL EXCAVATION

Figure 2 illustrates model tunnel in a typical centrifuge test (i.e., Test B). It can be seen that the model tunnel consists of five independent cylindrical rubber bags. Each rubber bag was filled with de-aired water which can be regarded as incompressible. Three-dimensional tunnel advancement was simulated in-flight by draining away a controlled amount of water from each rubber bag one by one. The amount of water drained away from each rubber bag is equivalent to a volume loss of 1% of the total volume of water in each rubber bag.

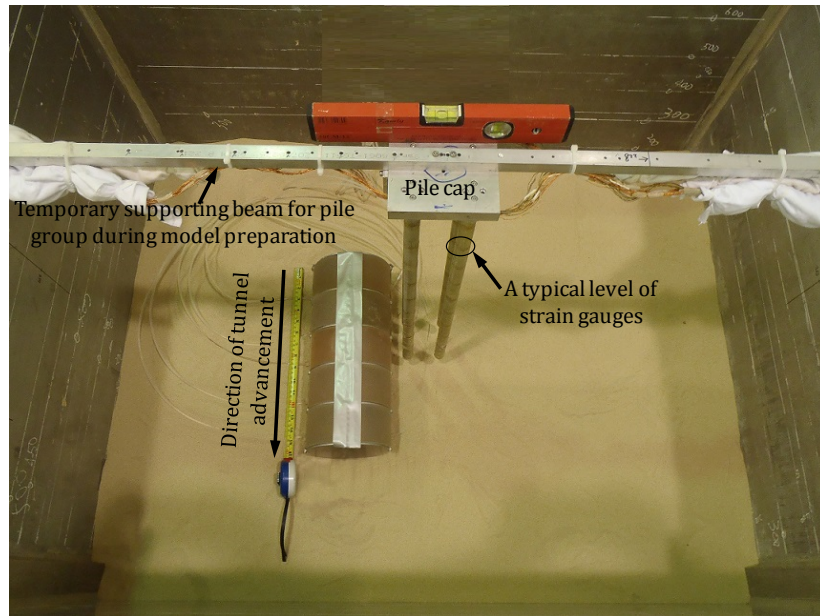


Figure 2: A typical model (Test B) set up showing model tunnel and pile group.

### 2.3. MODEL PILE GROUP AND INSTRUMENTATION

As shown in Figure 2, a 2×2 pile group was located at the centre of model container. Each model pile was fabricated from a 600 mm (24 m in prototype) long aluminium tube with an outer and inner diameter of 20 mm and 15 mm, respectively. Each model pile corresponds to a 0.8 m diameter (in prototype) cylindrical reinforced concrete (grade 40, reinforcement ratio = 1%) pile with flexural stiffness and bending moment capacity of 721 M Nm<sup>2</sup> and 800 kNm, respectively. The embedded depth for each pile was 490 mm (see Fig. 1) which corresponds to 19.6 m in prototype scale. To measure the axial force due to tunnelling, each model pile was instrumented with semiconductor strain gauges (SGs) bonded on external surface of the pile, at ten levels, at a spacing of 60 mm (2.4 m in prototype scale). At each level, full Wheatstone bridge strain gauges were arranged for temperature compensation.

### 2.4. MODEL PREPARTION AND TESTING PROCEDURE

Dry Toyoura sand was used in the tests. The specific gravity ( $G_s$ ) of sand grains is 2.65. The minimum and maximum void ratio ( $e_{min}$  and  $e_{max}$ ) of Toyoura sand are 0.977 and 0.597, respectively (Ishihara, 1993). Sand was rained into strongbox from a hopper at a constant height of 500 mm. A fairly uniform density of 1532 kg/m<sup>3</sup> (i.e.  $D_r = 65\%$ ) was achieved in both tests. After model preparation, dead weight (i.e. 8.6 kg) was put on top of pile cap. The whole model package was then mounted onto the swinging platform and spun up to 40 g. Upon reaching 40 g, in-flight tunnel excavation was simulated. The tunnel excavation was simulated in five stages, by draining away water from five rubber bags with a 1.0% volume loss for each. The induced settlement of pile group, tilting of pile cap and axial load along each pile were recorded during each stage of advancement.

## 3. THREE-DIMENSIONAL NUMERICAL BACK-ANALYSIS

In addition to the centrifuge testing, numerical back-analyses were carried out using the finite element program ABAQUS (Hibbitt et al. 2008).

### 3.1. FINITE ELEMENT MESH AND BOUNDARY CONDITIONS

Figure 3a and 3b show plan and elevation view of a typical finite element mesh (for back-analysing test T), respectively. To facilitate direct comparison between the measured and computed results, all dimensions of the finite-element mesh were in model scale and were identical to those in the centrifuge tests. The soil and the deadweight were modelled with eight-node brick elements while the pile was modelled with four-node shell elements. The boundaries adopted in the finite element analysis consisted of roller supports applied to vertical sides and pin supports applied to the base of the mesh.

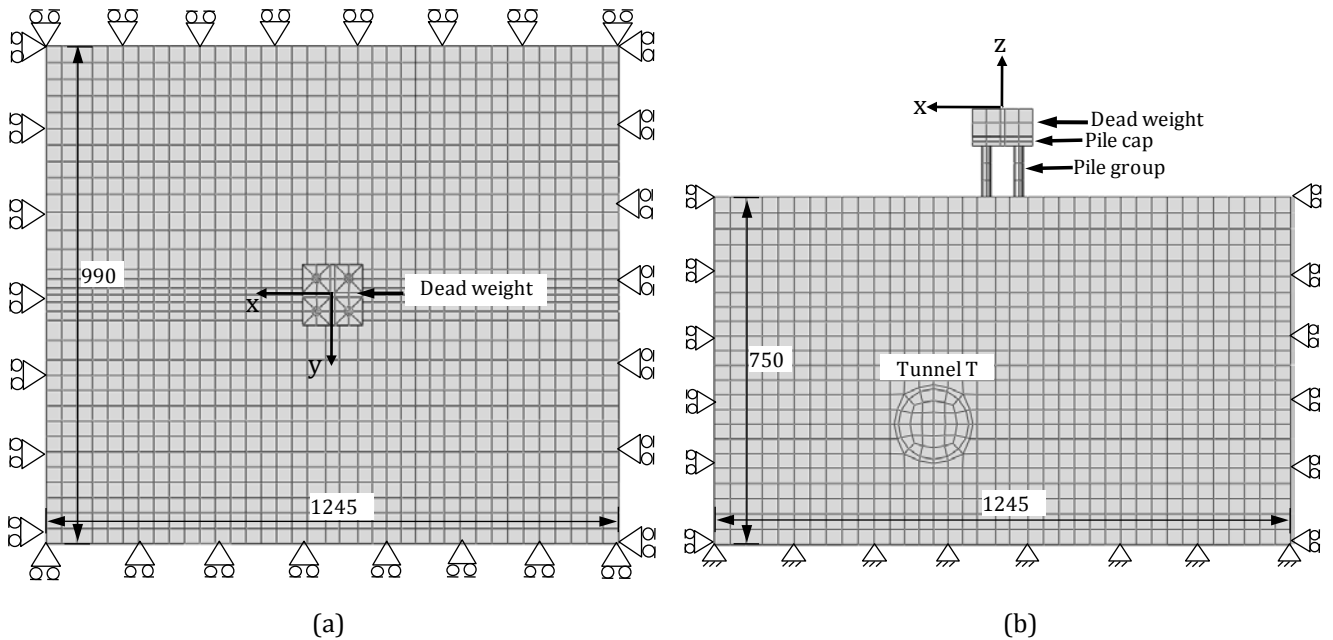


Figure 3: Finite element mesh for Test T. (a) Plan view (b) Elevation view (All dimensions are in mm)

### 3.2. CONSTITUTIVE MODEL AND MODEL PARAMETERS

A hypoplastic constitutive model with small strain stiffness was adopted in this study to model dry Toyoura sand. Hypoplastic constitutive models were developed to describe the nonlinear response of granular material (Gudehus (1996); Mašín (2012)). An intergranular strain concept or small strain stiffness has been incorporated into hypoplastic constitutive models (Niemunis and Herle 1997). Herle and Gudehus (1999) reported calibration results of model parameters ( $\phi'_c$ ,  $h_s$ ,  $n$ ,  $e_{do}$ ,  $e_{co}$ , and  $e_{io}$ ) for Toyoura sand. Triaxial test results of Maeda and Miura (1999) were used to determine exponent  $\alpha$  and  $\beta$  by curve fitting. Small strain stiffness or intergranular strain concept parameters ( $m_R$ ,  $m_T$ ,  $R$ ,  $\beta_r$ , and  $\chi_r$ ) were calibrated by curve fitting the triaxial test results with local strain measurements of Yamashita et al. (2000). The coefficient of earth pressure at-rest,  $K_0$  was assumed to be 0.5. The model parameters are summarized in Table 1.

Table 1: Model parameters of Toyoura sand adopted in the numerical back-analysis

Decription	Parameter	Reference
Effective angle of shearing resistance at critical state: $\phi$	$31^\circ$	Ishihara (1993)
Coefficient of at-rest earth pressure, $K_0$	0.5	Estimated by Jáký (1944)'s equation
Hardness of granulates, $h_s$	2.6GPa	
Exponent, $n$	0.27	Herle & Gudehus (1999)
Minimum void ratio at zero pressure, $e_{do}$	0.61	
Maximum void ratio at zero pressure, $e_{io}$	1.1	
Critical void ratio at zero pressure, $e_{co}$	0.98	
Exponent $\alpha$	0.14	
Exponent $\beta$	3	Calibrated from stiffness degradation curve of Toyoura sand (Yamashita et al., 2000)
Parameter controlling initial shear modulus upon $180^\circ$ strain path reversal, $m_R$	8	
Parameter controlling initial shear modulus upon $90^\circ$ strain path reversal, $m_T$	4	
Size of elastic range, $R$	$2 \times 10^{-5}$	
Parameter controlling degradation rate of stiffness with strain, $\beta_r$	0.1	
Parameter controlling degradation rate of stiffness with strain, $\chi_r$	1.0	

### 3.3. NUMERICAL MODELLING PROCEDURE

Procedures of numerical analysis are the same as those of the centrifuge tests. Details are summarized as follows:

Step 1: Set up the initial conditions at 1g (geostatic stress conditions with  $K_0=0.5$ , initial value of void ratio and intergranular strain) with boundary conditions defined in section 3.1.

Step 2: Activate the elements representing pile group (modelled as 'wished-in-place') and the deadweight on the pile cap.

Step 3: Increase stress level of soil, pile group and deadweight by specifying gravitational acceleration from 1g to 40g.

Step 4: Simulate the advancement of the tunnel by specifying zero horizontal displacement at the tunnel face of the tunnel segment to be excavated, excavate the soil inside the segment by deactivating soil elements inside it. Simultaneously, the tunnel lining is erected by activating it. The annulus gap between the tunnel lining and the soil excavated is equivalent to 1% volume loss.

Step 5: Repeat step 4 to excavate the next segment and install appropriate tunnel lining until the last (fifth) segment is completed.

## 4. INTERPRETATION OF MEASURED AND COMPUTED RESULTS

All measured and computed results are presented in prototype scale unless stated otherwise.

### 4.1. PILE GROUP SETTLEMENT WITH ADVANCEMENT OF THE TUNNEL

Figure 4 compares the induced measured and computed pile group settlement ( $S_p$ ) during advancement of the tunnel in both tests (i.e., Test T and B). The settlement and the distance from tunnel face to centre of the pile group ( $y$ ) are normalized by pile diameter ( $d_p$ ) and tunnel diameter ( $D$ ), respectively. In centrifuge tests, the induced settlement was measured by a LVDT mounted on the center of dead weight.

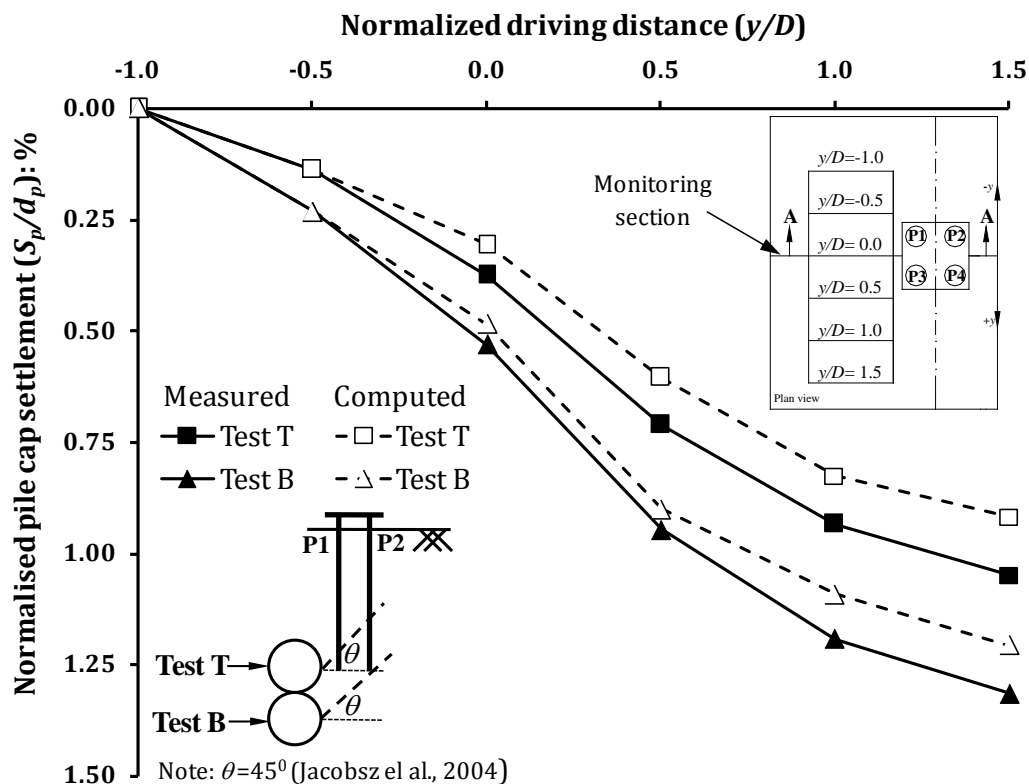


Figure 4: Normalised measured and computed pile group settlement at various stages of tunnelling.

It can be seen from the figure that the pile group starts to settle as the tunnel advances in each test. The rate of settlement increased as the tunnel face approached the monitoring section (i.e.,  $y/D=0$ ) but reduced as soon as the tunnel face moved pass that section. During entire process of tunnelling, the  $S_p$

induced due to tunnel B is always greater than tunnel T. Because in case of Test B, entire pile group is located within major influence zone due to tunnelling. Jacobs et al (2004) identified from their centrifuge tests in dry sand the major zone of influence as a result of tunnelling. They found that tunnelling-induced ground movement in sand was mostly confined to a region bounded by wedges with an angle of inclination of  $45^\circ$  extending from the tunnel springline to the ground surface.

The pile group experienced total settlements (due to working load and tunnelling) of 32.5, and 34.5 (i.e. 4.1, 4.3% of pile diameter) in tests T and B, respectively. Zhang & Ng (2005) proposed a reliability-based serviceability criterion for settlement (i.e. 56 mm), based on information from 95 settling buildings. Their criterion suggests that after the tunnelling in both tests, the pile group still satisfied the serviceability requirement.

The computed  $S_p$  in the two tests show similar trends as compared with measured data. Quantitatively, the maximum difference between the measured and the computed  $S_p$  is not more than 10%.

#### 4.2. TILTING OF PILE CAP IN TRANSVERSE DIRECTION OF THE TUNNEL

Figure 5 shows the tilting of pile cap in the transverse direction of tunnel advancement during excavations of the tunnel in Test T and Test B. LVDTs L2 and L3 were installed on the top of dead weight to measure the settlements at two different locations on the dead weight, as shown in Fig. 1. Tilting is defined as the ratio of differential settlement between measured by the LVDTs (L2 & L3) to the distance between them.

It can be observed from Figure 5 that as the tunnel advances towards monitoring section; the pile cap starts to tilt towards the tunnel in both the tests. During the first excavation stage (i.e.  $y/D = -1.0$  to  $-0.5$ ), the pile cap tilting is quite small. However, when the tunnel face reaches between  $y/D = -0.5$  and  $1.0$ , the pile cap tilts significantly towards the tunnel as a result of stress release due to these excavation stages. The most critical stage is when tunnel face is between  $y/D = -0.5$  and  $0.5$ , when the largest magnitude of incremental tilting is induced. Incremental tilting due to the fifth excavation (i.e.  $y/D = 1.0$  to  $1.5$ ) is only 0.014% and 0.006% in Test T and Test B, respectively. These non-linear observations cannot be captured in a centrifuge test carried out under the plane strain condition. During the entire process of the tunnelling, the largest tilting of the pile group always took place in Test T while the smallest always occurred in Test B. This response is the exact opposite of that in the tunnelling-induced settlement of the pile group as discussed in Fig. 4. After the tunnelling, the maximum tilting of the pile group (occurred in Test T) is about 0.2% (reaching the tilting limit recommended by Eurocode 7 (CEN, 2001) for high rise buildings). Compared to the measured tilting, the computed result shows reasonable agreement in both trend and magnitude. The maximum difference between the measurements and the computed results was 12%.

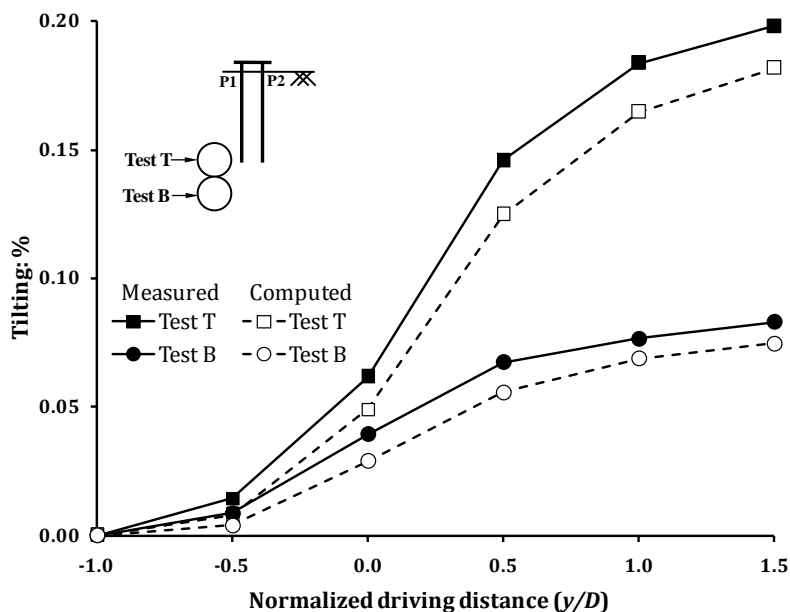


Figure 5: Measured and computed pile cap tilting in transverse direction due to tunnelling.

### 4.3. LOAD TRANSFER MECHANISM AT VARIOUS STAGES OF THE TUNNEL EXCAVATION

To understand the load sharing mechanism between the pile shaft and the pile toe, the load taken by the pile shaft ( $P_s$ ) is normalized by the total load carried by the pile head ( $P_h$ ). A load sharing ratio ( $P_s/P_h$  ratio) equal to 1 means the head load is fully transferred to the pile shaft (i.e., friction pile) while a  $P_s/P_h$  ratio equal to 0 represents the head load is entirely resisted by the pile toe (i.e., end bearing pile). Figure 6 shows the measured and computed change of the load sharing ratio of pile P1 with tunnelling stages in Tests T and B.

It can be seen from the measured results that before tunnelling (after application of working load), about 46% of the load acting on P1 was carried by the pile shaft. In Test T, the load sharing ratio kept decreasing during the entire process of the tunnelling. At the end of the tunnelling T, only about 26% of the total load acting on pile P1 was taken by the pile shaft. This suggests there was a downward load transfer from pile shaft to the pile toe. The load carried by pile toe increased to 74%. In Test B, the measured load sharing ratio increased during the tunnelling, suggesting a downward load the tunneling stages. At the end of the tunnelling B, about 66% of the total load acting on the pile P1 was carried by the pile shaft. Therefore, the tunnel B caused a larger settlement of the pile group than the tunnel T. The computed loading sharing ratios were comparable to the computed ones.

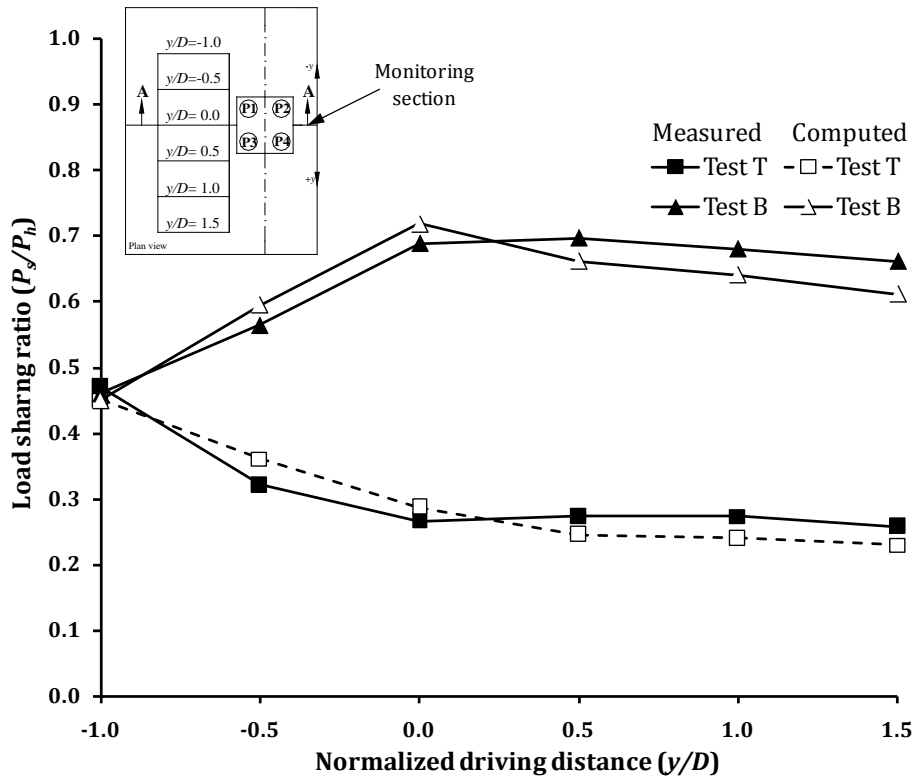


Figure 6: Measured and computed load sharing between the shaft and the toe of pile P1 in Test T and Test B.

### 4.4. COMPUTED CHANGE IN VERTICAL STRESS UNDER THE PILE GROUP TOE.

To further support the discussion in the previous section, Fig. 7 shows the computed change of vertical effective stress ( $\sigma_v'$ ) in the soil immediately below the toe of the pile group (along section A-A) due to tunnelling in both Tests T and B.

After tunnel excavation of tunnel T,  $\sigma_v'$  under both piles P1 and P2 increased. This suggested a further mobilisation of end-bearing of the pile group, in order to compensate the reduction in mobilised shaft resistance (see Fig. 6) due to tunnelling T. The increase in  $\sigma_v'$  below pile P1 (closer to the tunnel T) was larger than that below pile P2. After tunneling T,  $\sigma_v'$  underneath both piles P1 and P2 increased by 280 and 130 kPa, respectively. The non-uniform change (150 kPa) in  $\sigma_v'$  should have caused differential settlement between the two piles and hence tilting of the pile group (see Fig. 5).

In contrast to the tunnelling next to the pile toe in Test T, advancement of the tunnel B (below the pile toe) in Test B induced reductions in  $\sigma_v'$  underneath both piles P1 and P2, as a result of stress release by

the 1% volume loss. To compensate the decrease in end-bearing resistance of the pile group, it had to settle to mobilise shaft resistance (Fig. 6). At the end of tunnelling B, the reduction in  $\sigma'_v$  below the piles P1 and P2 were 92 and 65 kPa, respectively. The non-uniform change of  $\sigma'_v$  (60 kPa) below the pile group in Test B was less than that (150 kPa) in Test T. A smaller tilting (0.08%) was therefore resulted in the former test, compared to that (0.2%) induced in the latter.

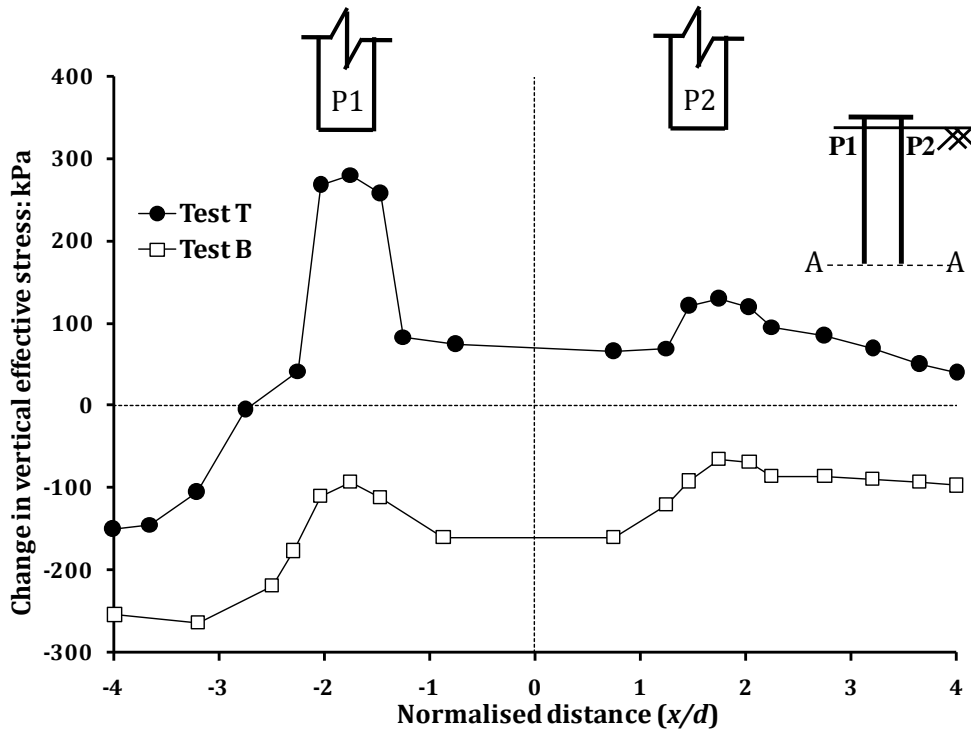


Figure 7: Computed change in vertical effective stress below the pile group due to tunnelling in tests T and B.

## 5. CONCLUSION

In this study, two centrifuge model tests and three-dimensional finite element back-analyses were carried out to investigate settlement and load transfer mechanism of a pile group subjected the tunnelling next to and below the toe of the pile group (Tests T and B, respectively). Based on the physical and numerical investigation, the following conclusions may be drawn:

(1) The tunnelling in test B caused the most significant settlement but the smallest differential settlement (i.e. tilting) of the pile group. This is because among the two tests conducted, the tunnelling in test B led to the most substantial but the most uniform reduction in vertical effective stress in the soil underneath the pile group. The cumulative settlements (due to working load and tunnelling) of the pile group resulting from the tunnelling in tests T and B were 32.5 and 34.5 mm, respectively.

(2) A much larger maximum transverse tilting was measured in test T (0.2%) than in test B (0.08%). This is because the tunnelling in test T led to the largest non-uniform change (150 kPa) in vertical effective stress underneath all piles in the group. The maximum tilting in test T reached the allowable limit (0.2%) suggested by Eurocode 7 (CEN, 2001).

(3) Two distinct load transfer mechanisms were identified, namely, downward load transfer (from pile shaft to pile toe) in test T and upward load transfer (from pile toe to pile shaft) in test B. Owing to the downward load transfer in test T, the load sharing ratio (load carried by the pile shaft divided by the total load acting on the pile) reduced from 46% before tunnelling to 26% after tunnelling. In contrast, the load sharing ratio of the pile in test B increased from 46% to 66% due to the upward load transfer.

## 6. ACKNOWLEDGEMENTS

The authors would like to acknowledge the financial supports from the Research Grants Council of the HKSAR (General Research Fund project numbers 617511 and 16207414), Quaid-e-Awam University of Engineering, Science and Technology, Sindh and Pakistan.

## REFERENCES

- [1] BEZUIJEN, A.; VAN DER SCHRIER, J. S. The influence of a bored tunnel on pile foundations. In Proceedings of centrifuge '94, pp. 681–686. Rotterdam, the Netherlands: Balkema.; 1994.
- [2] CEN. Eurocode 7, part 1: Geotechnical design: General rules, Final Draft prEN 1997-1. Brussels, Belgium: European Committee for Standardization (CEN) 2001.
- [3] GUDEHUS, G. A comprehensive constitutive equation for granular materials. Soils Found. 1996, 36 (1), 1–12.
- [4] HERLE, I. & GUDEHUS, G. (1999). Determination of parameters of a hypoplastic constitutive model from properties of grain assemblies. Mech. Cohesive Frictional Mater 1999, 4(5), 461–486.
- [5] HIBBITT, KARLSSON & SORENSEN. Inc. ABAQUS User's Manual, version 6.8.2; 2008.
- [6] ISHIHARA, K. Liquefaction and flow failure during earthquakes. Géotechnique 1993, 43(3) 351–415
- [7] JACOBSZ, S. W.; STANDING, J. R.; MAIR, R. J.; HAHIWARA, T.; SUIYAMA, T. Centrifuge modeling of tunnelling near driven piles. Soil Found. 2004, 44 (1), 49–56.
- [8] JÁKY, J. The coefficient of earth pressure at rest. J. Soc. Hungarian Architects Engrs 1944, 1, 355–358. (In Hungarian).
- [9] LEE, C. J.; CHIANG, K. H. Responses of single piles to tunnelling-induced soil movements in sandy ground. Can. Geotech. J. 2007, 44 (10), 1224–1241.
- [10] LOGANATHAN, N.; POULOS, H. G.; STEWART, D. P. Centrifuge model testing of tunnelling-induced ground and pile deformations. Geotechnique 2000, 50 (3), 283–294.
- [11] MAEDA, K.; MIURA, K. 1999. Relative density dependency of mechanical properties of sands. Soils and Foundations 1999, 39(1), 69–79.
- [12] MAŠÍN, D. 2012. Hypoplastic Cam-clay model. Géotechnique 2012, 62(6), 549–553.
- [13] MARSHALL, A. M.; MAIR, R. J. Tunneling beneath driven or jacked end-bearing piles in sand. Can. Geotech. J. 2011, 48 (12), 1757–1771.
- [14] NG, C. W. W.; LU, H.; PENG, S. Y. Three-dimensional centrifuge modelling of effects of twin tunnelling on an existing pile. Tunnelling Underground Space Technol. 2013, 35, 189–199.
- [15] NG, C. W. W.; SOOMRO, M. A.; HONG, Y. Three-dimensional centrifuge modelling of pile group responses to side-by-side twin tunnelling. Tunnelling Underground Space Technol. 2014, 43, 350–361.
- [16] NG, C. W. W. The 6th ZENG Guo-xi Lecture: the State-of-the-Art centrifuge modelling of geotechnical problems at HKUST. J Zhejiang Univ-Sci A (Applied Physics & Engineering) 2014, 15 (1), 1–21.
- [17] NIEMUNIS, A.; HERLE, I. 1997. Hypoplastic model for cohesionless soils with elastic strain range. Mechanics of Cohesive-Frictional Materials, 2: 279–299.
- [18] SOOMRO, M. A.; HONG, Y.; NG, C. W. W.; LU, H.; PENG, S. Y. Load transfer mechanism in pile group due to single tunnel advancement in stiff clay. Tunnelling Underground Space Technol. 2015, 45, 63–72.
- [19] YAMASHITA, S.; JAMIOLKOWSKI, M.; PRESTI, D.C.F.L. Stiffness nonlinearity of three sands. J. Geotech. Geoenviron. Eng. ASCE 2000, 126, 929–938.
- [20] Zhang, L. M. & Ng, A. M. Y. (2005). Probabilistic limiting tolerable displacements for serviceability limit state design of foundations. Géotechnique 2005, 55 (2), 151–161.

***Dr, Mukhtiar Ali, Soomro***  
***Quaid-e-Awam University of Science & Technology, Sindh, Pakistan***  
***E-mail address: eng.soomro@gmail.com***

***Associate Professor, David, Mašin***  
***Charles University in Prague, Czech Republic***  
***E-mail address: masin@natur.cuni.cz***

***Chair professor, Charles Wang Wai, Ng***  
***Hong Kong University of Science & Technology, HKSAR***  
***E-mail address: cecwwng@ust.hk***